Correlating resonant di-Higgs and tri-Higgs production to $H \to VV$ in the two-Higgs-doublet model

Guglielmo Coloretti,[1,*] Andreas Crivellin,[2,3,†] and Howard E. Haber[4,‡]

[1]*INFN, Sezione di Bologna, Via Irnerio 46, 40126 Bologna, Italy*
[2]*Universitat Autònoma de Barcelona, 08193 Bellaterra, Barcelona*
[3]*ICREA, Institució Catalana de Recerca i Estudis Avançats, Passeig de Lluís Companys 23, 08010 Barcelona, Spain*
[4]*Santa Cruz Institute for Particle Physics, University of California, 1156 High Street, Santa Cruz, California 95064, USA*

(Received 3 February 2026; accepted 26 June 2026; published 28 July 2026)

The observation of resonant di-Higgs production, which would strongly suggest the existence of a new heavy neutral scalar H, has been searched for extensively at the LHC. In the two-Higgs doublet model (2HDM) with $m_H \gg m_h$, where h is the Higgs boson of mass 125 GeV observed at the LHC, we show that a direct correlation emerges between $\mathrm{Br}(H \to hh)$ and $\mathrm{Br}(H \to VV)$, with $V = Z, W$, which depends only on m_H (and m_V). In particular, for heavy scalar masses between 500 GeV and 1 TeV, we find that $\mathrm{Br}(H \to hh)/\mathrm{Br}(H \to ZZ) \approx 9.4 \pm 0.25$. Moreover, $H \to hh$ is a dominant decay mode over a significant region of the parameter space and serves as the primary probe for a heavy scalar resonance at current and future hadron colliders. The origin of these predictions is most transparent in the Higgs basis, where the term in the scalar potential proportional to $\mathcal{H}_1^\dagger \mathcal{H}_1 \mathcal{H}_1^\dagger \mathcal{H}_2$ (and its Hermitian conjugate) generates the leading contributions to the Hhh and $Hhhh$ couplings in the decoupling limit of the 2HDM. Additionally, the latter coupling governs the resonant prompt tri-Higgs production via $H \to hhh$, which is also directly correlated to $H \to hh$ (and $H \to VV$), and can yield rates large enough to be measured at the High-Luminosity LHC.

DOI: 10.1103/g6sn-bf5n

I. INTRODUCTION

With the discovery of the Higgs boson at the LHC at CERN [1,2] (denoted by h with $m_h \simeq 125$ GeV), the spectrum of fundamental particles of the Standard Model (SM) is now completely observed. Moreover, the properties of the Higgs boson match the corresponding predictions of the SM within the experimental accuracy of the measurements [3–6].

Nevertheless, it is striking that the scalar sector employed by the SM is minimal, in contrast to the nonminimal structure of the fermionic sector that exhibits a replication of quark and lepton generations. One might therefore anticipate a nonminimal scalar sector in which the Higgs doublet field of the SM is replicated as well. Indeed, there are hints for the existence of new particles in general, and new Higgs bosons in particular, with masses of order 1 TeV and below [7]. Importantly, even if current hints for new physics at the LHC turn out to be statistical fluctuations, there is still ample motivation to study the phenomenological implications of extensions of the SM scalar sector.

A smoking-gun signature of extended Higgs sectors containing new scalars heavier than $2m_h$ is resonant di-Higgs production. This process has been studied in the context of multiple models (see Refs. [8,9] for a review), including the scalar singlet-extended SM [10–13], the two-Higgs doublet model (2HDM) [14–18] and more involved setups [19–21]. Indeed, resonant di-Higgs production is searched for extensively at the LHC in multiple channels [22–32], with a recent combination resulting in impressively strong limits on the corresponding cross section [33]. In the event of a future observation of resonant di-Higgs production, it is imperative to develop predictions that can distinguish among the various models.

In this article, we will examine resonant di-Higgs production in the context of the 2HDM, which was originally introduced in Ref. [34] and has been extensively developed and analyzed in the literature.[1] In light of the

*Contact author: guglielmo.coloretti@bo.infn.it
†Contact author: andreas.crivellin@icrea.cat
‡Contact author: haber@scipp.ucsc.edu

[1]For comprehensive reviews of the 2HDM, see, e.g., Refs. [35–37] and Chapter 6.2 of Ref. [38].

LHC Higgs data, which imply that the properties of h are approximately those of the SM Higgs boson [3–6], the parameters of the 2HDM must be consistent with the so-called Higgs alignment limit [39–46]. The Higgs alignment condition is naturally satisfied in the decoupling limit of the 2HDM [40,47], where all the new scalar states are significantly heavier than h, under the assumption of perturbative scalar self-couplings. In our analysis, we shall simplify the presentation by first neglecting possible new CP-violating effects in the scalar sector, with a focus on the production and decay of the heavy CP-even neutral scalar, denoted by H. A brief treatment of the CP-violating case will be given at the end of this work.

In the decoupling limit (where $m_H \gg m_h$), we will show that the 2HDM exhibits direct correlations of resonant di-Higgs production with $H \to VV$ ($V = W$ or Z) that depend only on m_H (and m_V). This feature can be most easily understood in the Higgs basis [48–53], where the Higgs vacuum expectation value (VEV) resides entirely in one of the two Higgs doublet fields. In the decoupling limit, the leading contribution to the Hhh coupling arises from a single term in the Higgs basis scalar potential, which is proportional to a parameter denoted by Z_6. Moreover, Z_6 also gives rise to the leading effect in resonant prompt tri-Higgs production ($pp \to H \to 3h$), where the first measurement attempts at the LHC have recently been made [54–56]. The cross sections for resonant di-Higgs and tri-Higgs production may be large enough to be observable at the High-Luminosity LHC (HL-LHC) [57,58] and FCC-hh [59,60].

II. 2HDM FORMALISM

The 2HDM employs two $\mathrm{SU}(2)_L$ complex scalar doublet fields Φ_1 and Φ_2, each with hypercharge $Y = \frac{1}{2}$. In general, the neutral components of the two doublet fields acquire VEVs, $\langle \Phi_i^0 \rangle = v_i/\sqrt{2}$, where $v_1 \equiv v c_\beta$ and $v_2 \equiv v s_\beta e^{i\xi}$, with $v \simeq 246$ GeV in a convention where $0 \le \beta \le \frac{1}{2}\pi$ and $0 \le \xi < 2\pi$, resulting in the breaking of the $\mathrm{SU}(2)_L \times \mathrm{U}(1)_Y$ gauge group to $\mathrm{U}(1)_{\mathrm{EM}}$.[2]

Without further assumptions, the choice of Φ_1–Φ_2 basis is arbitrary. It is therefore convenient to introduce the Higgs basis fields $\mathcal{H}_1$ and $\mathcal{H}_2$ (following Ref. [61]),

$$\mathcal{H}_1 = \begin{pmatrix} \mathcal{H}_1^+ \\ \mathcal{H}_1^0 \end{pmatrix} \equiv c_\beta \Phi_1 + s_\beta e^{-i\xi} \Phi_2, \tag{1}$$

$$\mathcal{H}_2 = \begin{pmatrix} \mathcal{H}_2^+ \\ \mathcal{H}_2^0 \end{pmatrix} = e^{i\eta}(-s_\beta e^{i\xi} \Phi_1 + c_\beta \Phi_2), \tag{2}$$

where the scalar potential is minimized so that only one of the scalar doublets acquires a nonzero VEV (i.e., $\langle \mathcal{H}_1^0 \rangle = v/\sqrt{2}$ and $\langle \mathcal{H}_2^0 \rangle = 0$). The complex phase factor $e^{i\eta}$ accounts for the nonuniqueness of the Higgs basis [61], since one is always free to rephase the Higgs doublet field whose vacuum expectation value vanishes.

In the Higgs basis, the most general renormalizable, $\mathrm{SU}(2)_L \times \mathrm{U}(1)_Y$ invariant scalar potential is given by

$$\begin{aligned}\mathcal{V} = {} & Y_1 \mathcal{H}_1^\dagger \mathcal{H}_1 + Y_2 \mathcal{H}_2^\dagger \mathcal{H}_2 + [Y_3 e^{-i\eta} \mathcal{H}_1^\dagger \mathcal{H}_2 + \mathrm{H.c.}] \\ & + \frac{1}{2} Z_1 (\mathcal{H}_1^\dagger \mathcal{H}_1)^2 + \frac{1}{2} Z_2 (\mathcal{H}_2^\dagger \mathcal{H}_2)^2 + Z_3 (\mathcal{H}_1^\dagger \mathcal{H}_1)(\mathcal{H}_2^\dagger \mathcal{H}_2) \\ & + Z_4 (\mathcal{H}_1^\dagger \mathcal{H}_2)(\mathcal{H}_2^\dagger \mathcal{H}_1) + \bigg\{ \frac{1}{2} Z_5 e^{-2i\eta} (\mathcal{H}_1^\dagger \mathcal{H}_2)^2 \\ & + [Z_6 e^{-i\eta} \mathcal{H}_1^\dagger \mathcal{H}_1 + Z_7 e^{-i\eta} \mathcal{H}_2^\dagger \mathcal{H}_2] \mathcal{H}_1^\dagger \mathcal{H}_2 + \mathrm{H.c.} \bigg\},\end{aligned} \tag{3}$$

where Y_1, Y_2, and $Z_1, \ldots, Z_4$ are real, whereas Y_3, Z_5, Z_6, and Z_7 are potentially complex parameters. The quantities Y_1 and Y_3 are fixed by the scalar potential minimization conditions,

$$Y_1 = -\frac{1}{2} Z_1 v^2, \qquad Y_3 = -\frac{1}{2} Z_6 v^2. \tag{4}$$

The Higgs basis fields couple to up-type and down-type fermions via the Yukawa coupling Lagrangian,

$$\begin{aligned}-\mathcal{L}_Y = {} & \bar{Q}(\hat{\boldsymbol{\kappa}}_{\boldsymbol{U}} \tilde{\mathcal{H}}_1 + \hat{\boldsymbol{\rho}}_{\boldsymbol{U}} \tilde{\mathcal{H}}_2) U + \bar{Q}(\hat{\boldsymbol{\kappa}}_{\boldsymbol{D}}^\dagger \mathcal{H}_1 + \hat{\boldsymbol{\rho}}_{\boldsymbol{D}}^\dagger \mathcal{H}_2) D \\ & + \bar{L}(\hat{\boldsymbol{\kappa}}_{\boldsymbol{E}}^\dagger \mathcal{H}_1 + \hat{\boldsymbol{\rho}}_{\boldsymbol{E}}^\dagger \mathcal{H}_2) E + \mathrm{H.c.},\end{aligned} \tag{5}$$

where $\tilde{\mathcal{H}}_k \equiv i\sigma_2 \mathcal{H}_k^*$ ($k = 1, 2$), and $\hat{\boldsymbol{\kappa}}_{\boldsymbol{F}}$ and $\hat{\boldsymbol{\rho}}_{\boldsymbol{F}}$ are 3×3 Yukawa matrices in flavor space ($F = U, D, E$) that are invariant with respect to scalar field basis transformations. The quark and lepton fields appear in left-handed $\mathrm{SU}(2)_L$ doublets Q and L, and right-handed $\mathrm{SU}(2)_L$ singlets U, D, and E (with the generation indices suppressed). When the fermion mass matrices $\hat{\boldsymbol{M}}_{\boldsymbol{F}} \equiv v \hat{\boldsymbol{\kappa}}_{\boldsymbol{F}}/\sqrt{2}$, are diagonalized via a singular value decomposition [62], the corresponding transformed $\hat{\boldsymbol{\rho}}_{\boldsymbol{F}}$ matrices are, in general, complex and nondiagonal, which can yield dangerously large tree-level flavor-changing neutral currents (FCNCs) mediated by neutral scalars (e.g., see Ref. [63] for a detailed analysis).

Here, we shall avoid off-diagonal neutral scalar couplings to fermions by imposing flavor alignment [64–72]. For this, we define (potentially complex) flavor-alignment parameters a_F in Eq. (5) via

$$\hat{\boldsymbol{\rho}}_{\boldsymbol{F}} = \frac{\sqrt{2}}{v} a_F \hat{\boldsymbol{M}}_{\boldsymbol{F}}, \quad \text{for } F = U, D, E, \tag{6}$$

where the a_F are invariant with respect to a change of the scalar field basis. As shown in Ref. [73], Eq. (6) is not

[2] We have employed the notation where $s_\beta \equiv \sin\beta$ and $c_\beta \equiv \cos\beta$. Without loss of generality, one is free to apply a suitable $\mathrm{U}(1)_Y$ transformation such that v is real and non-negative.

stable under renormalization group running except in special cases corresponding to the existence of a $\mathbb{Z}_2$ symmetry that is manifestly realized in a particular scalar field basis. This is the case of natural flavor conservation [74,75], which is often assumed in 2HDM phenomenological studies. However, to be more general, we do not make this assumption here, as phenomenological considerations do not require it.[3]

In light of the form of the scalar potential [Eq. (3)] and the flavor alignment condition [Eq. (6)], the scalar sector of the 2HDM yields potentially new sources of CP violation beyond the phase in the Cabibbo-Kobayashi-Maskawa (CKM) mixing matrix. To simplify the analysis presented in this work, we assume that all new sources of CP violation are absent. In particular, we shall assume that the flavor alignment parameters a_F defined in Eq. (6) are real. In addition, we shall also assume the existence of a real Φ_1–Φ_2 basis in which all the parameters of the scalar potential are real, and the corresponding scalar field VEVs are real (i.e., CP is not spontaneously broken by the scalar potential). It then follows that a real Higgs basis exists where the potentially complex scalar potential parameters Y_3, Z_5, Z_6, and Z_7 [cf. Eq. (3)] are all real, and $\sin\xi = \sin\eta = 0$ [cf. Eqs. (1) and (2)]. That is,

$$\xi, \eta = 0 \mod \pi. \tag{7}$$

Since $\sin\xi = 0$ in a real Φ_1–Φ_2 basis, it follows that $s_\beta e^{\pm i\xi} = s_\beta \cos\xi = \pm s_\beta$. Thus, it is convenient to redefine $s_\beta \to s_\beta \mathrm{sgn}(\cos\xi)$, in which case the range of the parameter β is extended to $-\frac{1}{2}\pi \leq \beta \leq \frac{1}{2}\pi$.

In particular, Y_3, Z_6, Z_7, and

$$\varepsilon \equiv e^{i\eta} = \cos\eta = \pm 1 \tag{8}$$

are real quantities that transform under a real orthogonal basis transformation, $\Phi_i \to \mathcal{R}_{ij}\Phi_j$, as

$$[Y_3, Z_6, Z_7, \varepsilon] \to \det\mathcal{R}[Y_3, Z_6, Z_7, \varepsilon], \tag{9}$$

with $\det\mathcal{R} = \pm 1$. In contrast, note that Z_5 is invariant under $\Phi_i \to \mathcal{R}_{ij}\Phi_j$. The quantity $\varepsilon = \pm 1$ accounts for the twofold nonuniqueness of the real Higgs basis. The parameter Z_6 plays a critical role in our analysis, and we shall henceforth assume that $Z_6 \neq 0$. In light of Eq. (9), it follows that εZ_6 is invariant under a real orthogonal basis transformation.

The neutral Higgs sector of the 2HDM consists of two CP-even neutral scalars, h_1 and h_2, with masses m_1 and m_2, respectively, and a CP-odd neutral scalar, $h_3 = \sqrt{2}\,\mathrm{Im}\,\mathcal{H}_2^0$, with mass $m_3 \equiv m_A$, where

$$m_A^2 = Y_2 + \frac{1}{2}(Z_3 + Z_4 - Z_5)v^2. \tag{10}$$

The two neutral CP-even Higgs scalars are identified by diagonalizing a 2×2 matrix, which is shown below [71] with respect to the basis $\{\sqrt{2}\mathrm{Re}\mathcal{H}_1^0 - v, \sqrt{2}\mathrm{Re}\mathcal{H}_2^0\}$,

$$\mathcal{M}^2 = \begin{pmatrix} Z_1 v^2 & \varepsilon Z_6 v^2 \\ \varepsilon Z_6 v^2 & m_A^2 + Z_5 v^2 \end{pmatrix}, \tag{11}$$

with corresponding mass eigenstates

$$h_1 = \left(\sqrt{2}\mathrm{Re}\mathcal{H}_1^0 - v\right)\cos\theta_{12} - \sqrt{2}\mathrm{Re}\mathcal{H}_2^0 \sin\theta_{12}, \tag{12}$$

$$h_2 = \left(\sqrt{2}\mathrm{Re}\mathcal{H}_1^0 - v\right)\sin\theta_{12} + \sqrt{2}\mathrm{Re}\mathcal{H}_2^0 \cos\theta_{12}, \tag{13}$$

and masses $m_i \equiv m_{h_i}$ (where $m_1 < m_2$) given by

$$m_{1,2}^2 = \frac{1}{2}\left[m_A^2 + (Z_1 + Z_5)v^2 \mp \sqrt{[m_A^2 + (Z_5 - Z_1)v^2]^2 + 4|Z_6|^2 v^4}\right], \tag{14}$$

in a notation where $m_1^2 < m_2^2$. The mixing angle θ_{12} is defined modulo π; by convention, we take $\cos\theta_{12} \geq 0$ and $-\frac{1}{2}\pi \leq \theta_{12} \leq \frac{1}{2}\pi$. In particular [81],

$$\sin\theta_{12} = \frac{\varepsilon Z_6 v^2}{\sqrt{(m_2^2 - m_1^2)(m_2^2 - Z_1 v^2)}}, \tag{15}$$

$$\cos\theta_{12} = \sqrt{\frac{m_2^2 - Z_1 v^2}{m_2^2 - m_1^2}}. \tag{16}$$

That is, θ_{12} is basis invariant and is thus independent of the twofold nonuniqueness of the real Higgs basis.

In light of the LHC Higgs data [3–6], one of the two neutral CP-even Higgs bosons must resemble the SM Higgs boson. Indeed, if $\varphi \equiv \sqrt{2}\mathrm{Re}\mathcal{H}_1^0 - v$ were a mass eigenstate, its tree-level couplings would precisely match those of the SM Higgs boson. The limiting case just described is known as the Higgs alignment limit [39–46] and corresponds to $\sin\theta_{12} = 0$ if the lighter of the two CP-even Higgs bosons, h_1, is identified with the Higgs scalar discovered at the LHC [14]. In particular, h_1 then resides entirely in the doublet $\mathcal{H}_1$ as indicated by Eq. (12).

The notation introduced above differs from the standard notation employed in the 2HDM literature [35,36], which was developed starting from a real Φ_1–Φ_2 basis where both the neutral components of Φ_1 and Φ_2 acquire a nonzero

[3]Flavor-aligned extended Higgs sectors can arise naturally from symmetries of ultraviolet completions of low-energy effective theories of flavor as shown in Refs. [76–78]. In such models, departures from exact flavor alignment due to renormalization group running down to the electroweak scale are typically small enough [79,80] to be consistent with all known FCNC bounds.

VEV. The diagonalization of the CP-even neutral scalar squared-mass matrix in this basis yields a mixing angle denoted by α. Neither α nor β has a separate physical meaning in a general 2HDM [62]. However, after returning to the Higgs basis, one finds [71]

$$\begin{pmatrix} H \\ h \end{pmatrix} = \begin{pmatrix} c_{\beta-\alpha} & -s_{\beta-\alpha} \\ s_{\beta-\alpha} & c_{\beta-\alpha} \end{pmatrix} \begin{pmatrix} \sqrt{2}\mathrm{Re}\mathcal{H}_1^0 - v \\ \varepsilon\sqrt{2}\mathrm{Re}\mathcal{H}_2^0 \end{pmatrix}, \tag{17}$$

where we have introduced the notation $s_{\beta-\alpha} \equiv \sin(\beta-\alpha)$ and $c_{\beta-\alpha} \equiv \cos(\beta-\alpha)$. Comparing the equation above with Eqs. (12) and (13), it follows that

$$\cos\theta_{12} = s_{\beta-\alpha}, \qquad \sin\theta_{12} = -\varepsilon\, c_{\beta-\alpha}, \tag{18}$$

or equivalently $\beta-\alpha = \varepsilon\theta_{12} + \frac{1}{2}\pi$. Since θ_{12} is invariant with respect to real orthogonal basis transformations, it follows that $s_{\beta-\alpha} \geq 0$, whereas $c_{\beta-\alpha}$ changes sign under an improper real orthogonal basis change [cf. Eq. (9)].

Moreover, the neutral scalar mass eigenstates typically employed in the 2HDM literature [35,36] are related to the basis-invariant fields h_i as follows [18,71]:

$$h = h_1, \qquad H = -\varepsilon\, h_2, \qquad A = \varepsilon\, h_3. \tag{19}$$

Similarly, the charged Higgs scalar field employed in the 2HDM literature is given by $H^\pm = \varepsilon\mathcal{H}_2^\pm$. The corresponding charged Higgs mass is

$$m_{H^\pm}^2 = Y_2 + \frac{1}{2}Z_3 v^2 = m_A^2 - \frac{1}{2}v^2(Z_4 - Z_5). \tag{20}$$

The scalar sector of the CP-conserving 2HDM is governed by the following eight independent parameters: $\{v, m_h, m_H, m_A, m_{H^\pm}, Z_2, Z_3, Z_7\}$. Note that the other Z_i are fixed:

$$Z_1 v^2 = m_h^2\, s_{\beta-\alpha}^2 + m_H^2\, c_{\beta-\alpha}^2, \tag{21}$$

$$Z_4 v^2 = m_h^2\, c_{\beta-\alpha}^2 + m_H^2\, s_{\beta-\alpha}^2 + m_A^2 - 2m_{H^\pm}^2, \tag{22}$$

$$Z_5 v^2 = m_h^2\, c_{\beta-\alpha}^2 + m_H^2\, s_{\beta-\alpha}^2 - m_A^2, \tag{23}$$

$$Z_6 v^2 = (m_h^2 - m_H^2) c_{\beta-\alpha} s_{\beta-\alpha}. \tag{24}$$

As h is identified with the SM-like Higgs boson observed at the LHC, it then follows that $|\sin\theta_{12}| \ll 1$ (or equivalently $|c_{\beta-\alpha}| \ll 1$).[4] In light of Eq. (15), the Higgs alignment limit can be achieved when $|Z_6| \ll 1$ and/or when $m_H \gg m_h$ (under the assumption that Z_6 lies in the perturbative regime). In this paper, we propose to examine the 2HDM where $|Z_6| \lesssim \mathcal{O}(1)$ and $Y_2 \gg v^2$, corresponding to the decoupling limit [40,62]. In this limit, $m_H \sim m_A \sim m_{H^\pm} \gg m_h$, or more precisely

$$m_h^2 = Z_1\, v^2 + \mathcal{O}\left(\frac{v^4}{m_A^2}\right), \tag{25}$$

$$m_H^2 = m_A^2 + Z_5\, v^2 + \mathcal{O}\left(\frac{v^4}{m_A^2}\right). \tag{26}$$

Moreover, Eqs. (15) and (18) yield $Z_6 c_{\beta-\alpha} < 0$, with

$$c_{\beta-\alpha} = -\frac{Z_6 v^2}{m_H^2} + \mathcal{O}\left(\frac{v^4}{m_A^4}\right). \tag{27}$$

III. DECAYS OF H AND A

The Feynman rule for the $HV_\mu V_\nu$ coupling, where $VV = W^+W^-$ or ZZ, is given by $ig_{HVV}g_{\mu\nu}$, with [35]

$$g_{HVV} = \frac{2m_V^2}{v} c_{\beta-\alpha}, \quad \text{for } V = W, Z. \tag{28}$$

As expected, the HVV couplings are suppressed close to the Higgs alignment limit, where $|c_{\beta-\alpha}| \ll 1$. There are no tree-level AVV couplings.

Next, we record the coupling of H to scalar final states. The only possible kinematically allowed H decay final states in the limit of new heavy Higgs boson masses $m_H \sim m_A \sim m_{H^\pm}$, where $m_H \gg v$, are hh and hhh. The corresponding Feynman rules for the Hhh and $Hhhh$ interaction vertices are given by ig_{Hhh} and ig_{Hhhh}, respectively, where [18,40,83]

$$g_{Hhh} = -3v\Big[Z_1\, c_{\beta-\alpha}s_{\beta-\alpha}^2 + Z_{345}c_{\beta-\alpha}\left(\frac{1}{3} - s_{\beta-\alpha}^2\right) - Z_6 s_{\beta-\alpha}(1-3c_{\beta-\alpha}^2) - Z_7 c_{\beta-\alpha}^2 s_{\beta-\alpha}\Big], \tag{29}$$

$$g_{Hhhh} = -3\Big[Z_1 s_{\beta-\alpha}^3 c_{\beta-\alpha} - Z_2 s_{\beta-\alpha}c_{\beta-\alpha}^3 + Z_{345}s_{\beta-\alpha}c_{\beta-\alpha}(c_{\beta-\alpha}^2 - s_{\beta-\alpha}^2) - Z_6 s_{\beta-\alpha}^2(1-4c_{\beta-\alpha}^2) - Z_7 c_{\beta-\alpha}^2(4s_{\beta-\alpha}^2 - 1)\Big], \tag{30}$$

with $Z_{345} \equiv Z_3 + Z_4 + Z_5$. In the decoupling limit, where $|Z_6| \lesssim \mathcal{O}(1)$ and $|c_{\beta-\alpha}| \ll 1$ [as a result of Eq. (27)], the scalar couplings above simplify to $g_{Hhh} \simeq 3vZ_6$ and $g_{Hhhh} \simeq 3Z_6$. Using Eq. (27), it follows that

$$\frac{g_{HVV}}{g_{Hhh}} \simeq -\frac{2m_V^2}{3m_H^2}. \tag{31}$$

[4]Experimental evidence for $|c_{\beta-\alpha}| \ll 1$ is provided in Ref. [82].

The partial decay rates of $H \to VV$ and $H \to hh$ are directly correlated at leading order in v^2/m_H^2. In particular, the corresponding partial decay rates of H into WW, ZZ, hh, and hhh are given by

$$\Gamma_{H\to VV} = c_V |g_{HVV}|^2 \frac{(m_H^4 - 4m_H^2 m_V^2 + 12 m_V^4)\sqrt{m_H^2 - 4m_V^2}}{64\pi m_V^4 m_H^2}, \quad \text{where } c_V = 1(1/2) \quad \text{for } V = W(Z), \tag{32}$$

$$\Gamma_{H\to hh} = \frac{1}{2!}|g_{Hhh}|^2 \frac{1}{16\pi m_H^2}\sqrt{m_H^2 - 4m_h^2}, \tag{33}$$

$$\Gamma_{H\to hhh} = \frac{1}{3!}|g_{Hhhh}|^2 \frac{1}{256\pi^3 m_H^3}\int_{4m_h^2}^{(m_H - m_h)^2} dx \lambda^{1/2}(x, m_H^2, m_h^2)\sqrt{1 - \frac{4m_h^2}{x}}, \tag{34}$$

where $\lambda(a,b,c) \equiv a^2 + b^2 + c^2 - 2ab - 2ac - 2bc$, and we have made use of results given in Refs. [35,84] and Appendix D of Ref. [38]. There are no decays of A to scalar final states due to the assumed CP symmetry.

It is instructive to derive an approximate formula for $\Gamma(H \to hh)/\Gamma(H \to VV)$ in the limit where $|c_{\beta-\alpha}| \ll 1$ and $m_H \gg m_V, m_h$,

$$\frac{\Gamma(H\to hh)}{\Gamma(H\to VV)} \simeq \frac{9}{2c_V}\left[1 + \frac{2(3m_V^2 - m_h^2)}{m_H^2}\right]. \tag{35}$$

Equation (35) yields asymptotic ratios of 9:2:1 for the decay rates of H into the final states hh, W^+W^-, ZZ, respectively. The same asymptotic ratios were also obtained in Ref. [85] in an extended scalar sector via the Higgs portal due to dimension-5 scalar operators (a phenomenon dubbed the busy Higgs mechanism). However, higher-dimensional operators are not needed in the 2HDM to reproduce the corresponding busy Higgs signal asymptotic ratios of Ref. [85].

Likewise, in the limit where $|c_{\beta-\alpha}| \ll 1$ and $m_H \gg m_h$,

$$\frac{\Gamma(H\to hhh)}{\Gamma(H\to hh)} \simeq \frac{m_H^2}{96\pi^2 v^2}\left\{1 - \frac{4m_h^2}{m_H^2}\left[1 - 3\ln\left(\frac{2m_h}{m_H}\right)\right]\right\}, \tag{36}$$

which is a factor of four smaller than the corresponding busy Higgs result with dimension-5 scalar operators.

Next, we exhibit the couplings of H and A to quarks and leptons via the Yukawa Lagrangian [71,80]:

$$\mathcal{L}_Y = \frac{1}{v}\sum_{F=U,D,E} \bar{F}\boldsymbol{M_F}[\varepsilon\, a_F\, s_{\beta-\alpha} - c_{\beta-\alpha}]F\, H, \tag{37}$$

$$+ \frac{i\varepsilon}{v}\left\{a_U \bar{U}\boldsymbol{M_U}\gamma_5 U - \sum_{F=D,E} a_F \bar{F}\boldsymbol{M_F}\gamma_5 F\right\}A, \tag{38}$$

where ε is defined in Eq. (8) and the $\boldsymbol{M_F}$ ($F = U, D, E$) are the corresponding diagonal up-type quark, down-type quark, and charged lepton mass matrices, respectively. The corresponding Feynman rules for the $Hf\bar{f}$ and $Af\bar{f}$ vertices are given by $ig_{Hf\bar{f}}$ and $ig_{Af\bar{f}}$, where

$$g_{Hf\bar{f}} = \frac{m_f}{v}(\varepsilon\, a_F\, s_{\beta-\alpha} - c_{\beta-\alpha}), \tag{39}$$

$$g_{Af\bar{f}} = \pm\frac{m_f}{v} i\varepsilon a_F \gamma_5, \tag{40}$$

where the upper [lower] sign in Eq. (40) corresponds to up-type (down-type) fermions, respectively. The partial decay rates of H and A into $t\bar{t}$ are given by

$$\Gamma(H \to t\bar{t}) = |g_{Ht\bar{t}}|^2 \frac{3m_H}{8\pi}\left(1 - \frac{4m_t^2}{m_H^2}\right)^{3/2}, \tag{41}$$

$$\Gamma(A \to t\bar{t}) = |g_{At\bar{t}}|^2 \frac{3m_A}{8\pi}\left(1 - \frac{4m_t^2}{m_A^2}\right)^{1/2}. \tag{42}$$

In the limit where $|c_{\beta-\alpha}| \ll 1$ and $m_H \gg m_t, m_h$,

$$\frac{\Gamma(H\to hh)}{\Gamma(H\to t\bar{t})} \simeq \frac{3v^4 Z_6^2}{4m_H^2 m_t^2 (a_U - \epsilon c_{\beta-\alpha})^2} \times \left[1 + \frac{2(3m_t^2 - m_h^2)}{m_H^2}\right], \tag{43}$$

where Z_6 is fixed by Eq. (24).

Under an improper real orthogonal basis transformation, the couplings g_{HVV}, g_{Hhh}, g_{Hhhh}, $g_{Hf\bar{f}}$, and $g_{Af\bar{f}}$ in change sign, as expected in light of Eqs. (18) and (19). Of course, the relevant physical quantities are the squares of these couplings, which are manifestly basis invariant.

Finally, we remark that one can set $\varepsilon = 1$, thereby fixing the real Higgs basis, as no observable depends on this choice.[5] Since $Z_6 c_{\beta-\alpha} < 0$ [cf. Eq. (27)], the signs of Z_6 and $c_{\beta-\alpha}$ are now physical but correlated. Moreover, due to the form of the $Hf\bar{f}$ coupling, it suffices to consider only positive values of $c_{\beta-\alpha}$ in a parameter space scan while allowing for values of a_F of either sign.

[5]This choice is implicitly made in most treatments of the CP-conserving 2HDM in the literature.

IV. PHENOMENOLOGICAL ANALYSIS

First, we examine the correlations among the decay widths (or equivalently, the branching ratios) given analytically in Sec. III. The red curve in Fig. 1 depicts the ratio $\Gamma(H \to hh)/\Gamma(H \to ZZ)$, and the blue curve depicts the ratio $\Gamma(H \to hhh)/\Gamma(H \to ZZ)$, as a function of m_H. In the mass range of 500 GeV $< m_H <$ 1 TeV, Eqs. (35) and (36) yield $9.65 \gtrsim \Gamma(H \to hh)/\Gamma(H \to ZZ) \gtrsim 9.15$ and $0.01 \lesssim \Gamma(H \to hhh)/\Gamma(H \to ZZ) \lesssim 0.1$. The approximate expressions used in obtaining Fig. 1 are reliable under the assumption that the self-coupling parameters $|Z_i| \lesssim \mathcal{O}(1)$ and $|c_{\beta-\alpha}| \ll 1$, which implies that the mass splittings among the heavy Higgs scalars are small [in light of Eqs. (21)–(23)]. Moreover, in the decoupling regime where $m_H \gg v$, Eq. (24) implies that $|Z_6| \sim (m_H^2/v^2) \times |c_{\beta-\alpha}| \gg |c_{\beta-\alpha}|$. Consequently, the exact expressions for the ratios of partial decay rates exhibited in Fig. 1 are insensitive to the specific choices for the other Z_i due to the $c_{\beta-\alpha}$ suppressions in Eqs. (29) and (30). Hence, the results of Fig. 1 can be used in the future to test the 2HDM in case any of the processes mentioned above are observed.

Next, we consider the relevant constraints on H production and decay in the decoupling regime. In this setup, the vector boson fusion production cross section is suppressed. However, the second Higgs doublet $\mathcal{H}_2$ couples to top quarks [cf. Eq. (5)], which induces gluon fusion production of A and H via a top quark loop. Using Eq. (39) with $\varepsilon = 1$, the gluon fusion cross section $gg \to H$ is given by

$$\sigma(gg \to H) = [a_U s_{\beta-\alpha} - c_{\beta-\alpha}]^2 \sigma(gg \to H_{\rm SM}), \qquad (44)$$

where $H_{\rm SM}$ is a hypothetical scalar with a mass of m_H and with couplings to gauge bosons and fermions that coincide with those of the SM Higgs boson.

For $m_H > 500$ GeV, the dominant and most sensitive decay channels are $\Gamma_{H\to ZZ}$ [cf. Eq. (32)], $\Gamma_{H\to hh}$ [cf. Eq. (33)], and $\Gamma_{H\to t\bar{t}}$. In light of Eqs. (39) and (41),

$$\Gamma_{H\to t\bar{t}} = [a_U s_{\beta-\alpha} - c_{\beta-\alpha}]^2 \Gamma_{H_{\rm SM}\to t\bar{t}}. \qquad (45)$$

The relevant experimental bounds can be found for $H, A \to t\bar{t}$ in Refs. [86,87], for $H \to ZZ$ in Refs. [88,89] and for $H \to hh$ in Ref. [33]. We have examined a benchmark point with $m_H = m_A = m_{H^\pm} = 800$ GeV, with Z_1, Z_4, Z_5, and Z_6 fixed via Eqs. (21)–(24). We have also set $Z_2 = Z_3 = Z_7 = 1$, although our results are quite insensitive to the specific choices for Z_2, Z_3, and Z_7, as previously indicated. For this benchmark point, $t\bar{t}$ searches give a limit of $|a_U s_{\beta-\alpha} - c_{\beta-\alpha}| \lesssim 0.5$ for H with $\Gamma_H/m_H = 1\%$[6] and $|a_U| \lesssim 0.4$ for A. For the $H \to ZZ$ decay channel with $m_H = 800$ GeV, the currently observed LHC upper limit is $\sigma(gg \to H) \times {\rm Br}[H \to ZZ] \approx 0.01$ pb, and for $H \to hh$, the upper limit is $\sigma(gg \to H) \times {\rm Br}[H \to hh] \approx 0.01$ pb.[7]

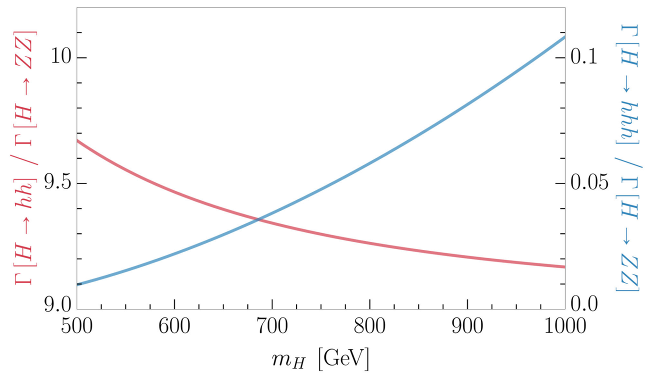

FIG. 1. 2HDM predictions for $\Gamma(H \to hh)/\Gamma(H \to ZZ)$ (left axis, red) and $\Gamma(H \to hhh)/\Gamma(H \to ZZ)$ (right axis, blue) using the approximate expressions for the ratios of partial decay widths given in Eqs. (35) and (36).

The results of our analysis are shown in Fig. 2. Currently, for $m_H = 800$ GeV, $H \to hh$ provides stronger constraints than $H \to ZZ$ over the whole parameter space. Furthermore, in light of Eq. (36), the cross section for prompt resonant tri-Higgs production $\sigma(pp \to H \to hhh)$ can be as large as 0.1 fb (2 fb) for $\sqrt{s} = 14$ TeV (100 TeV) [99], which may be observable at the HL-LHC (100 TeV FCC-hh) with an integrated luminosity of 3000 fb^{-1} (20 ab^{-1}). Focusing on the most sensitive tri-Higgs production channel, the $6b$ final state, with a b-jet efficiency of $\epsilon_b \approx 0.85$ and a cut efficiency[8] of $\epsilon_{\rm cut} \approx 0.1$ (0.0115) [101], one can expect up to 3 (35) events.

In the allowed parameter space, the resonant decay $H \to hh$ can compete with $H \to t\bar{t}$ and can even become the dominant decay mode. This behavior, which is a consequence of Eq. (43), is highlighted within the region bounded by the dot-dashed lines in Fig. 2. Indeed, the branching ratio of $H \to hh$ can exceed 70% in some regions of the parameter space, as shown in Fig. 3. As noted below Eq. (45), the LHC di-Higgs measurements constrain the production cross section to a value that is no larger than 0.01 pb. In particular, the di-Higgs production cross section is compatible with a relatively small top-quark alignment parameter a_U, which suppresses the $H \to t\bar{t}$ decay mode as indicated in Eq. (43).

[6]We checked that for the allowed parameter space, the ratio Γ_H/m_H does not exceed 5%.

[7]The searches for $t\bar{t}$ associated production of A and H [90,91] as well as the charged Higgs in tb associated production ($pp \to tbH^\pm$) with $H^\pm \to tb$ [92–98] do not yield competitive bounds.

[8]The cut efficiency is derived from a cut-based analysis, while more recent studies based on deep learning techniques achieve an improvement by a factor of 6 resulting in approximately 18 events at the HL-LHC [100].

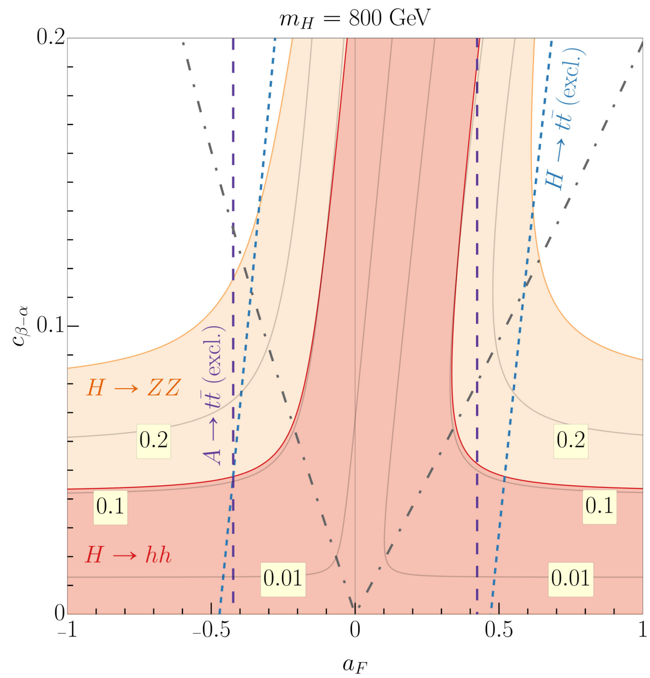

Fig. . Continues on facing page.

FIG. 2. Allowed regions in the a_F vs $c_{\beta-\alpha}$ plane for $m_H = m_A = m_{H^\pm} = 800$ GeV, where $a_F \equiv a_U = a_D = a_E$. The contour lines show $\sigma(pp \to H \to hhh)$ in units of femtobarns for $\sqrt{s} = 14$ TeV. The regions outside the dashed lines are excluded by $H \to t\bar{t}$ (blue) and $A \to t\bar{t}$ (violet) searches at the LHC. In the region that lies inside the two dot-dashed lines, $H \to hh$ is the dominant decay mode [cf. Eqs. (35) and (43) with $\epsilon = 1$]. Note that in the decoupling limit with $|Z_6| \lesssim 1$ Eq. (27) implies that $|c_{\beta-\alpha}| \lesssim 0.1$.

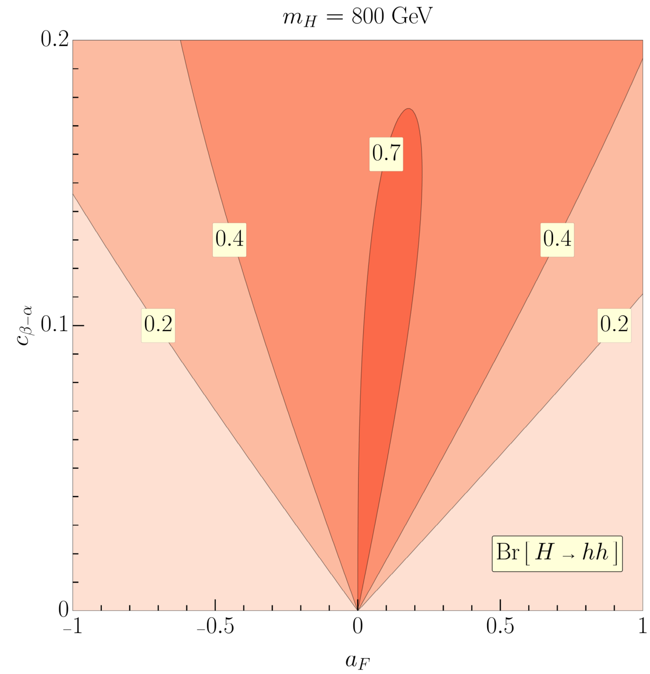

FIG. 3. The branching ratio of $H \to hh$ in the a_F vs $c_{\beta-\alpha}$ plane for $m_H = m_A = m_{H^\pm} = 800$ GeV, where $a_F \equiv a_U = a_D = a_E$ and $\epsilon = 1$ [cf. Eq. (43)]. Contour lines corresponding to a branching ratio of 0.2, 0.4, and 0.7 are exhibited.

Note that the relations among the direct search channels discussed above hold at tree level and are sensitive to loop corrections [102]. However, for $\mathcal{O}(1)$ self-couplings in the scalar potential, the loop effects are small. Furthermore, the constraints imposed by the LHC Higgs data are, in general, satisfied close to the Higgs alignment limit. In particular, the deviation of the $h \to \gamma\gamma$ signal strength from the predicted value in the SM is mainly sensitive to Z_3 (via the charged Higgs boson loop), which does not significantly affect the tree-level observables analyzed in this paper. Finally, perturbativity constraints are easily satisfied by choosing appropriately small mass splittings among H, A and $H^\pm$.

V. EFFECTS OF *CP* VIOLATION

Although the analysis of Sec. IV was carried out in the context of the *CP*-conserving 2HDM, our conclusions hold even in the case where additional sources of *CP* violation are present.[9] This can be seen as follows: in the *CP*-violating 2HDM, the three neutral scalar mass eigenstates are states of indefinite *CP*, denoted by h_1, h_2, and h_3. We adopt the convention where $m_1 < m_2, m_3$ (where $m_k \equiv m_{h_k}$) and assume that h_1 can be identified with the SM-like Higgs boson h observed at the LHC. Indeed, in the Higgs alignment limit, h_1 is approximately *CP* even, whereas h_2 and h_3 are not *CP* eigenstates. The three neutral scalar mass eigenstates are obtained by diagonalizing a 3×3 squared-mass matrix, and as shown in Refs. [61,62], the diagonalization procedure yields two physical mixing angles, denoted by θ_{12} and θ_{13}.

In the decoupling limit where $m_2 \sim m_3 \sim m_{H^\pm} \gg v$, Eq. (27) is replaced by [18]

$$\sin\theta_{12} = \frac{v^2 \mathrm{Re}(Z_6 e^{-i\eta})}{m_2^2} + \mathcal{O}\left(\frac{v^4}{m_2^4}\right), \tag{46}$$

$$\sin\theta_{13} = -\frac{v^2\, \mathrm{Im}(Z_6 e^{-i\eta})}{m_3^2} + \mathcal{O}\left(\frac{v^4}{m_3^4}\right). \tag{47}$$

The couplings of h_k to VV, hh, and hhh in the decoupling limit are given at leading order by

$$g_{h_k VV} \simeq \frac{2m_V^2}{v} \sin\theta_{1k}, \quad \text{for } k = 2, 3, \tag{48}$$

$$g_{h_2 hh} \simeq -3v \mathrm{Re}(Z_6 e^{-i\eta}), \tag{49}$$

$$g_{h_3 hh} \simeq 3v\, \mathrm{Im}(Z_6 e^{-i\eta}), \tag{50}$$

$$g_{h_2 hhh} \simeq -3 \mathrm{Re}(Z_6 e^{-i\eta}), \tag{51}$$

[9] One must check that the parameters of the *CP*-violating 2HDM are not in conflict with the current experimental constraints [103] on the electric dipole moment of the electron [104].

$$g_{h_3hhh} \simeq 3\,\mathrm{Im}(Z_6 e^{-i\eta}). \tag{52}$$

In particular, in light of Eqs. (46) and (47), we obtain

$$\frac{g_{h_kVV}}{g_{h_khh}} \simeq -\frac{2m_V^2}{3m_k^2}, \quad \text{for } k = 2, 3, \tag{53}$$

which generalizes the result of Eq. (31).

Similarly, the couplings of h_2 and h_3 to fermions are obtained from the Yukawa Lagrangian at leading order in the decoupling limit,

$$\begin{aligned}\mathcal{L}_Y = &-\frac{1}{v}\bigg\{\bar{U}\boldsymbol{M_U}(a^U P_R + a^{U*}P_L) \\ &+ \sum_{F=D,E}\bar{F}\boldsymbol{M_F}(a^{F*}P_R + a^F P_L)\bigg\}h_2 \\ &- \frac{i}{v}\bigg\{\bar{U}\boldsymbol{M_U}(-a^U P_R + a^{U*}P_L) \\ &+ \sum_{F=D,E}\bar{F}\boldsymbol{M_F}(a^{F*}P_R - a^F P_L)\bigg\}h_3,\end{aligned} \tag{54}$$

where $P_{R,L} \equiv \frac{1}{2}(1 \pm \gamma_5)$ and the flavor-alignment parameters a^F ($F = U$, D, E) may be complex. However, the magnitude of the corresponding couplings of h_2 and h_3 to fermion pairs will not differ significantly from the corresponding CP-conserving case.

Therefore, in the CP-violating 2HDM, the analysis of Sec. IV can be applied to resonant di-Higgs and tri-Higgs production via resonant h_2 and h_3 production and decay,[10] where $|Z_6|$ is replaced by the basis-independent scalar self-couplings $\mathrm{Re}(Z_6 e^{-i\eta})$ and $\mathrm{Im}(Z_6 e^{-i\eta})$, respectively. Note that the decay $h_2 \to \gamma\gamma$ [$h_3 \to \gamma\gamma$] is mediated at one loop primarily via the couplings of h_2 [h_3] to W^+W^-, $t\bar{t}$, and H^+H^-, where the latter is proportional to $\mathrm{Re}(Z_7 e^{-i\eta})$ [$\mathrm{Im}(Z_7 e^{-i\eta})$], respectively [107,108]. However, the corresponding h_2 and h_3 decay widths are negligible in the region of parameter space considered in this work.

[10] The interplay between the Higgs alignment limit of the 2HDM and CP-violating observables has been studied via nonresonant cascade di-Higgs and tri-Higgs production in Refs. [105,106].

VI. CONCLUSIONS

In this paper, we have derived simple relations among the decay widths of the heavier CP-even Higgs boson of the 2HDM (denoted by H) into hh, ZZ, WW, and hhh that hold for $m_H \gg v$, i.e., close to the Higgs alignment limit in the decoupling regime. In particular, we find that $9.65 \gtrsim \Gamma(H \to hh)/\Gamma(H \to ZZ) \gtrsim 9.15$ and $0.01 \lesssim \Gamma(H \to hhh)/\Gamma(H \to ZZ) \lesssim 0.1$ when 500 GeV $< m_H <$ 1 TeV. These relations can be used as simple tests of the 2HDM if a new scalar particle is discovered in one of these decay modes. Furthermore, by taking into account the current experimental LHC bounds on $H \to ZZ$, $H \to hh$, $H \to t\bar{t}$, and $A \to t\bar{t}$, we find that a significant region of the parameter space exists where $H \to hh$ is a dominant decay mode and serves as the leading probe for the discovery of a heavy scalar narrow resonance at current and future hadron colliders. Furthermore, $\sigma(pp \to H \to hhh)$ can be as large as 0.1 fb at $\sqrt{s} = 14$ TeV, thereby suggesting that resonant prompt tri-Higgs production in a 2HDM might be observable at the HL-LHC (with better prospects at a future FCC-hh collider at $\sqrt{s} = 100$ TeV).

ACKNOWLEDGMENTS

G. C. and H. E. H. thank Zhen Liu for an illuminating discussion of his recent work and the relation of our result to the busy Higgs signal introduced in Ref. [85] subsequent to our paper. A. C. and G. C. acknowledge support from a professorship grant from the Swiss National Science Foundation (Grant No. PP00P21_76884). H. E. H. is supported in part by the U.S. Department of Energy Grant No. DE-SC0010107.

DATA AVAILABILITY

The data are not publicly available. The data are available from the authors upon reasonable request.

[1] G. Aad et al. (ATLAS Collaboration), Observation of a new particle in the search for the Standard Model Higgs boson with the ATLAS detector at the LHC, Phys. Lett. B **716**, 1 (2012).

[2] S. Chatrchyan et al. (CMS Collaboration), Observation of a new boson at a mass of 125 GeV with the CMS experiment at the LHC, Phys. Lett. B **716**, 30 (2012).

[3] G. Add et al. (ATLAS Collaboration), A detailed map of Higgs boson interactions by the ATLAS experiment ten years after the discovery, Nature (London) **607**, 52 (2022); **612**, E24(E) (2022); **623**, E5(E) (2023).

[4] ATLAS Collaboration, Combined measurements of Higgs boson production and decay at $\sqrt{s} = 13$ TeV using up to 140 fb^{-1} of data collected by the ATLAS Experiment,

ATLAS-CONF-2025-006, 2025, https://inspirehep.net/files/5a7c1be57465f55ad7e69ab07bc1d66c.

[5] A. Tumasyan *et al.* (CMS Collaboration), A portrait of the Higgs boson by the CMS experiment ten years after the discovery, Nature (London) **607**, 60 (2022); **623**, E4(E) (2023).

[6] A. Hayrapetyan *et al.* (CMS Collaboration), Combined measurements and interpretations of Higgs boson production and decay in proton-proton collisions at $\sqrt{s} = 13$ TeV, arXiv:2602.18611.

[7] A. Crivellin and B. Mellado, Anomalies in particle physics and their implications for physics beyond the standard model, Nat. Rev. Phys. **6**, 294 (2024).

[8] M. Mühlleitner, M. O. P. Sampaio, R. Santos, and J. Wittbrodt, Phenomenological comparison of models with extended Higgs sectors, J. High Energy Phys. 08 (2017) 132.

[9] H. Abouabid, A. Arhrib, D. Azevedo, J. E. Falaki, P. M. Ferreira, M. Mühlleitner, and R. Santos, Benchmarking di-Higgs production in various extended Higgs sector models, J. High Energy Phys. 09 (2022) 011.

[10] V. Barger, P. Langacker, M. McCaskey, M. Ramsey-Musolf, and G. Shaughnessy, Complex singlet extension of the Standard Model, Phys. Rev. D **79**, 015018 (2009).

[11] R. Costa, M. Mühlleitner, M. O. P. Sampaio, and R. Santos, Singlet extensions of the standard model at LHC Run 2: Benchmarks and comparison with the NMSSM, J. High Energy Phys. 06 (2016) 034.

[12] S. Dawson and M. Sullivan, Enhanced di-Higgs boson production in the complex Higgs singlet model, Phys. Rev. D **97**, 015022 (2018).

[13] J. M. No and M. Spannowsky, Signs of heavy Higgs bosons at CLIC: An e^+e^- road to the Electroweak Phase Transition, Eur. Phys. J. C **79**, 467 (2019).

[14] J. Bernon, J. F. Gunion, H. E. Haber, Y. Jiang, and S. Kraml, Scrutinizing the alignment limit in two-Higgs-doublet models: $m_h = 125$ GeV, Phys. Rev. D **92**, 075004 (2015).

[15] B. Grzadkowski, H. E. Haber, O. M. Ogreid, and P. Osland, Heavy Higgs boson decays in the alignment limit of the 2HDM, J. High Energy Phys. 12 (2018) 056.

[16] F. Kling, S. Su, and W. Su, 2HDM Neutral Scalars under the LHC, J. High Energy Phys. 06 (2020) 163.

[17] F. Arco, S. Heinemeyer, M. Mühlleitner, and K. Radchenko, Sensitivity to triple Higgs couplings via di-Higgs production in the 2HDM at the (HL-)LHC, Eur. Phys. J. C **83**, 1019 (2023).

[18] H. E. Haber, V. Keus, and R. Santos, P-even, *CP*-violating signals in scalar-mediated processes, Phys. Rev. D **106**, 095038 (2022).

[19] M. Maniatis, The next-to-minimal supersymmetric extension of the Standard Model reviewed, Int. J. Mod. Phys. A **25**, 3505 (2010).

[20] K. Hartling, K. Kumar, and H. E. Logan, The decoupling limit in the Georgi-Machacek model, Phys. Rev. D **90**, 015007 (2014).

[21] W.-J. Zhang, W.-G. Ma, R.-Y. Zhang, X.-Z. Li, L. Guo, and C. Chen, Double Higgs boson production and decay in Randall-Sundrum model at hadron colliders, Phys. Rev. D **92**, 116005 (2015).

[22] G. Aad *et al.* (ATLAS Collaboration), Combination of searches for Higgs boson pairs in pp collisions at $\sqrt{s} = 13$ TeV with the ATLAS detector, Phys. Lett. B **800**, 135103 (2020).

[23] G. Aad *et al.* (ATLAS Collaboration), Search for Higgs boson pair production in the two bottom quarks plus two photons final state in pp collisions at $\sqrt{s} = 13$ TeV with the ATLAS detector, Phys. Rev. D **106**, 052001 (2022).

[24] G. Aad *et al.* (ATLAS Collaboration), Search for resonant pair production of Higgs bosons in the $b\bar{b}b\bar{b}$ final state using pp collisions at $\sqrt{s} = 13$ TeV with the ATLAS detector, Phys. Rev. D **105**, 092002 (2022).

[25] G. Aad *et al.* (ATLAS Collaboration), Search for resonant and non-resonant Higgs boson pair production in the $b\bar{b}\tau^+\tau^-$ decay channel using $\sqrt{s} = 13$ TeV pp collision data from the ATLAS detector, J. High Energy Phys. 07 (2023) 040.

[26] G. Aad *et al.* (ATLAS Collaboration), Search for Higgs boson pair production in association with a vector boson in pp collisions at $\sqrt{s} = 13$ TeV with the ATLAS detector, Eur. Phys. J. C **83**, 519 (2023).

[27] G. Aad *et al.* (ATLAS Collaboration), Search for pair production of boosted Higgs bosons via vector-boson fusion in the $b\bar{b}b\bar{b}$ final state using pp collisions at $\sqrt{s} = 13$ TeV with the ATLAS detector, Phys. Lett. B **858**, 139007 (2024).

[28] A. M. Sirunyan *et al.* (CMS Collaboration), Combination of searches for Higgs boson pair production in proton-proton collisions at $\sqrt{s} = 13$ TeV, Phys. Rev. Lett. **122**, 121803 (2019).

[29] A. Tumasyan *et al.* (CMS Collaboration), Search for Higgs boson pairs decaying to WW^*WW^*, $WW^*\tau\tau$, and $\tau\tau\tau\tau$ in proton-proton collisions at $\sqrt{s} = 13$ TeV, J. High Energy Phys. 07 (2023) 095.

[30] A. Tumasyan *et al.* (CMS Collaboration), Search for a new resonance decaying into two spin-0 bosons in a final state with two photons and two bottom quarks in proton-proton collisions at $\sqrt{s} = 13$ TeV, J. High Energy Phys. 05 (2024) 316.

[31] A. Hayrapetyan *et al.* (CMS Collaboration), Search for a new heavy scalar resonance decaying into the Higgs boson and a new scalar particle in the $b\bar{b}b\bar{b}$ final state using proton-proton collisions at $\sqrt{s} = 13$ TeV, arXiv:2605.02848.

[32] A. Hayrapetyan *et al.* (CMS Collaboration), Search for the nonresonant and resonant production of a Higgs boson in association with an additional scalar boson in the $\gamma\gamma\tau\tau$ final state in proton-proton collisions at $\sqrt{s} = 13$ TeV, J. High Energy Phys. 05 (2026) 186.

[33] G. Aad *et al.* (ATLAS Collaboration), Combination of searches for resonant Higgs boson pair production using pp collisions at s = 13 TeV with the ATLAS detector, Phys. Rev. Lett. **132**, 231801 (2024).

[34] T. D. Lee, A theory of spontaneous T violation, Phys. Rev. D **8**, 1226 (1973).

[35] J. F. Gunion, H. E. Haber, G. L. Kane, and S. Dawson, *The Higgs Hunter's Guide* (Westview Press, Boulder, CO, 2000).

[36] G. C. Branco, P. M. Ferreira, L. Lavoura, M. N. Rebelo, M. Sher, and J. P. Silva, Theory and phenomenology of two-Higgs-doublet models, Phys. Rep. **516**, 1 (2012).

[37] I. P. Ivanov, Building and testing models with extended Higgs sectors, Prog. Part. Nucl. Phys. **95**, 160 (2017).
[38] H. K. Dreiner, H. E. Haber, and S. P. Martin, *From Spinors to Supersymmetry* (Cambridge University Press, Cambridge, England, 2023).
[39] I. F. Ginzburg, M. Krawczyk, and P. Osland, Potential of photon collider in resolving SM like scenarios, Nucl. Instrum. Methods Phys. Res., Sect. A **472**, 149 (2001).
[40] J. F. Gunion and H. E. Haber, The *CP* conserving two Higgs doublet model: The Approach to the decoupling limit, Phys. Rev. D **67**, 075019 (2003).
[41] N. Craig and S. Thomas, Exclusive signals of an extended Higgs sector, J. High Energy Phys. 11 (2012) 083.
[42] N. Craig, J. Galloway, and S. Thomas, Searching for signs of the second Higgs doublet, arXiv:1305.2424.
[43] D. M. Asner *et al.*, ILC Higgs White Paper, in *Snowmass 2013: Snowmass on the Mississippi*, 2013, https://arxiv.org/pdf/1310.0763.
[44] M. Carena, I. Low, N. R. Shah, and C. E. M. Wagner, Impersonating the Standard Model Higgs Boson: Alignment without decoupling, J. High Energy Phys. 04 (2014) 015.
[45] H. E. Haber, The Higgs data and the decoupling limit, in *Proceedings of the 1st Toyama International Workshop on Higgs as a Probe of New Physics*, edited by S. Kanemura and T. Shindou, pp. 32–46, http://www3.u-http://www3.u-toyama.ac.jp/theory/HPNP2013/HPNP2013Proceedings.pdf.
[46] P. S. Bhupal Dev and A. Pilaftsis, Maximally symmetric two Higgs doublet model with natural Standard Model alignment, J. High Energy Phys. 12 (2014) 024; 11 (2015) 147(E).
[47] H. E. Haber and Y. Nir, Multiscalar models with a high-energy scale, Nucl. Phys. **B335**, 363 (1990).
[48] H. Georgi and D. V. Nanopoulos, Suppression of flavor changing effects from neutral spinless meson exchange in gauge theories, Phys. Lett. **82B**, 95 (1979).
[49] L. Lavoura, Signatures of discrete symmetries in the scalar sector, Phys. Rev. D **50**, 7089 (1994).
[50] L. Lavoura and J. P. Silva, Fundamental *CP* violating quantities in a $SU(2) \times U(1)$ model with many Higgs doublets, Phys. Rev. D **50**, 4619 (1994).
[51] F. J. Botella and J. P. Silva, Jarlskog-like invariants for theories with scalars and fermions, Phys. Rev. D **51**, 3870 (1995).
[52] G. C. Branco, L. Lavoura, and J. P. Silva, *CP Violation* (Oxford University Press, Oxford, 1999).
[53] S. Davidson and H. E. Haber, Basis-independent methods for the two-Higgs-doublet model, Phys. Rev. D **72**, 035004 (2005); **72**, 099902(E) (2005).
[54] CMS Collaboration, Search for triple Higgs pro- duction in Run2 data of CMS using $4b2\gamma$ final state, CMS-PAS-HIG-24-015, 2025, https://cds.cern.ch/record/2937680/files/HIG-24-015-pas.pdf.
[55] CMS Collaboration, Search for nonresonant triple Higgs boson production in the six b-quark final state in proton-proton collisions at $\sqrt{s} = 13$ TeV, CMS-PAS-HIG-24-012, 2025, https://cds.cern.ch/record/2945361/files/HIG-24-012-pas.pdf.
[56] G. Aad *et al.* (ATLAS Collaboration), Search for triple Higgs boson production in the 6b final state using pp collisions at $\sqrt{s} = 13$ TeV with the ATLAS detector, Phys. Rev. D **111**, 032006 (2025).
[57] G. Apollinari *et al.*, editors, High-Luminosity Large Hadron Collider (HL-LHC): Technical Design Report V. 0.1, CERN Yellow Report 4/2017 (2017) 10.23731/CYRM-2017-004.
[58] M. Cepeda *et al.*, Report from working group 2: Higgs physics at the HL-LHC and HE-LHC, CERN Yellow Rep. Monogr. **7**, 221 (2019).
[59] M. L. Mangano, editor, Physics at the FCC-hh, a 100 TeV pp collider, CERN Yellow Report 3/2017 (2017) 10.23731/CYRM-2017-003.
[60] A. Abada *et al.* (FCC Collaboration), FCC-hh: The hadron collider: Future circular collider conceptual design report Volume 3, Eur. Phys. J. Special Topics **228**, 755 (2019).
[61] R. Boto, T. V. Fernandes, H. E. Haber, J. C. Romão, and J. P. Silva, Basis-independent treatment of the complex 2HDM, Phys. Rev. D **101**, 055023 (2020).
[62] H. E. Haber and D. O'Neil, Basis-independent methods for the two-Higgs-doublet model. II. The significance of $\tan\beta$, Phys. Rev. D **74**, 015018 (2006); **74**, 059905(E) (2006).
[63] A. Crivellin, A. Kokulu, and C. Greub, Flavor-phenomenology of two-Higgs-doublet models with generic Yukawa structure, Phys. Rev. D **87**, 094031 (2013).
[64] A. Pich and P. Tuzon, Yukawa Alignment in the two-Higgs-doublet model, Phys. Rev. D **80**, 091702 (2009).
[65] A. Pich, Flavour constraints on multi-Higgs-doublet models: Yukawa alignment, Nucl. Phys. B, Proc. Suppl. **209**, 182 (2010).
[66] O. Eberhardt, A. P. Martínez, and A. Pich, Global fits in the aligned two-Higgs-doublet model, J. High Energy Phys. 05 (2021) 005.
[67] S. Y. Choi, J. S. Lee, and J. Park, Alignment of Yukawa couplings in two Higgs doublet models, arXiv:2011.04978.
[68] J. S. Lee and J. Park, Yukawa alignment revisited in the Higgs basis, Phys. Rev. D **106**, 015023 (2022).
[69] H. Serodio, Yukawa Alignment in a multi Higgs doublet model: An effective approach, Phys. Lett. B **700**, 133 (2011).
[70] G. Cree and H. E. Logan, Yukawa alignment from natural flavor conservation, Phys. Rev. D **84**, 055021 (2011).
[71] J. M. Connell, P. Ferreira, and H. E. Haber, Accommodating hints of new heavy scalars in the framework of the flavor-aligned two-Higgs-doublet model, Phys. Rev. D **108**, 055031 (2023).
[72] A. Karan, V. Miralles, and A. Pich, Updated global fit of the aligned two-Higgs-doublet model with heavy scalars, Phys. Rev. D **109**, 035012 (2024).
[73] P. M. Ferreira, L. Lavoura, and J. P. Silva, Renormalization-group constraints on Yukawa alignment in multi-Higgs-doublet models, Phys. Lett. B **688**, 341 (2010).
[74] S. L. Glashow and S. Weinberg, Natural conservation laws for neutral currents, Phys. Rev. D **15**, 1958 (1977).
[75] E. A. Paschos, Diagonal neutral currents, Phys. Rev. D **15**, 1966 (1977).
[76] S. Knapen and D. J. Robinson, Disentangling mass and mixing hierarchies, Phys. Rev. Lett. **115**, 161803 (2015).

[77] D. Egana-Ugrinovic, S. Homiller, and P. Meade, Aligned and spontaneous flavor violation, Phys. Rev. Lett. **123**, 031802 (2019).

[78] D. Egana-Ugrinovic, S. Homiller, and P. R. Meade, Higgs bosons with large couplings to light quarks, Phys. Rev. D **100**, 115041 (2019).

[79] C. B. Braeuninger, A. Ibarra, and C. Simonetto, Radiatively induced flavour violation in the general two-Higgs doublet model with Yukawa alignment, Phys. Lett. B **692**, 189 (2010).

[80] S. Gori, H. E. Haber, and E. Santos, High scale flavor alignment in two-Higgs doublet models and its phenomenology, J. High Energy Phys. 06 (2017) 110.

[81] H. E. Haber, A tale of three diagonalizations, Int. J. Mod. Phys. A **36**, 2130003 (2021).

[82] G. Aad *et al.* (ATLAS Collaboration), Interpretations of the ATLAS measurements of Higgs boson production and decay rates and differential cross-sections in pp collisions at $\sqrt{s} = 13$ TeV, J. High Energy Phys. 11 (2024) 097.

[83] H. E. Haber, "The two-Higgs-doublet model from the ground up" (to be published).

[84] E. Byckling and K. Kajante, *Particle Kinematics* (John Wiley & Sons Ltd., London, 1973).

[85] P. Li, Z. Liu, and L.-T. Wang, A busy Higgs signal, arXiv:2604.14284.

[86] A. Hayrapetyan *et al.* (CMS Collaboration), Search for heavy pseudoscalar and scalar bosons decaying to a top quark pair in proton–proton collisions at $\sqrt{s} = 13$ TeV, Rep. Prog. Phys. **88**, 127801 (2025).

[87] G. Aad *et al.* (ATLAS Collaboration), Search for heavy neutral Higgs bosons decaying into a top quark pair in 140 fb^{-1} of proton-proton collision data at $\sqrt{s} = 13$ TeV with the ATLAS detector, J. High Energy Phys. 08 (2024) 013.

[88] A. Hayrapetyan *et al.* (CMS Collaboration), Search for a new heavy scalar resonance decaying to a pair of Z bosons in the four-lepton final state in proton-proton collisions at $\sqrt{s} = 13$ TeV, arXiv:2605.26462.

[89] G. Aad *et al.* (ATLAS Collaboration), Search for heavy resonances decaying into a pair of Z bosons in the $\ell^+\ell^-\ell\prime^+\ell\prime^-$ and $\ell^+\ell^-\nu\bar{\nu}$ final states using 139 fb^{-1} of proton–proton collisions at $\sqrt{s} = 13$ TeV with the ATLAS detector, Eur. Phys. J. C **81**, 332 (2021).

[90] A. M. Sirunyan *et al.* (CMS Collaboration), Search for production of four top quarks in final states with same-sign or multiple leptons in proton-proton collisions at $\sqrt{s} = 13$ TeV, Eur. Phys. J. C **80**, 75 (2020).

[91] G. Aad *et al.* (ATLAS Collaboration), Search for $t\bar{t}H/A \to t\bar{t}t\bar{t}$ production in proton–proton collisions at $\sqrt{s} = 13$ TeV with the ATLAS detector, Eur. Phys. J. C **85**, 573 (2025).

[92] A. M. Sirunyan *et al.* (CMS Collaboration), Search for charged Higgs bosons in the $H^\pm \to \tau^\pm\nu_\tau$ decay channel in proton-proton collisions at $\sqrt{s} = 13$ TeV, J. High Energy Phys. 07 (2019) 142.

[93] A. Tumasyan *et al.* (CMS Collaboration), Search for a charged Higgs boson decaying into a heavy neutral Higgs boson and a W boson in proton-proton collisions at $\sqrt{s} = 13$ TeV, J. High Energy Phys. 09 (2023) 032.

[94] A. M. Sirunyan *et al.* (CMS Collaboration), Search for charged Higgs bosons produced in vector boson fusion processes and decaying into vector boson pairs in proton–proton collisions at $\sqrt{s} = 13$ TeV, Eur. Phys. J. C **81**, 723 (2021).

[95] A. Hayrapetyan *et al.* (CMS Collaboration), Search for charged Higgs bosons decaying into top and bottom quarks in lepton + jets final states in proton-proton collisions at $\sqrt{s} = 13$ TeV, arXiv:2512.24471.

[96] G. Aad *et al.* (ATLAS Collaboration), Search for charged Higgs bosons produced in top quark decays or in association with top quarks and decaying via $H^\pm \to \tau^\pm\nu_\tau$ in $\sqrt{s} = 13$ TeV pp collisions with the ATLAS detector, Phys. Rev. D **111**, 072006 (2025).

[97] G. Aad *et al.* (ATLAS Collaboration), Search for charged Higgs bosons decaying into a top quark and a bottom quark at $\sqrt{s} = 13$ TeV with the ATLAS detector, J. High Energy Phys. 06 (2021) 145.

[98] G. Aad *et al.* (ATLAS Collaboration), Search for a heavy charged Higgs boson decaying into a W boson and a Higgs boson in final states with leptons and b-jets in $\sqrt{s} = 13$ TeV pp collisions with the ATLAS detector, J. High Energy Phys. 02 (2025) 143.

[99] J. Baglio, A. Djouadi, and J. Quevillon, Prospects for Higgs physics at energies up to 100 TeV, Rep. Prog. Phys. **79**, 116201 (2016).

[100] C.-W. Chiang, F.-Y. Hsieh, S.-C. Hsu, Z.-Z. Li, and I. Low, Enhancing the sensitivity for triple Higgs boson searches with deep learning techniques, J. High Energy Phys. 03 (2026) 261.

[101] A. Papaefstathiou and G. Tetlalmatzi-Xolocotzi, Multi-Higgs boson production with anomalous interactions at current and future proton colliders, J. High Energy Phys. 06 (2024) 124.

[102] S. Heinemeyer, M. Mühlleitner, K. Radchenko, and G. R. Weiglein, Higgs Pair Production in the 2HDM: Impact of Loop Corrections to the Trilinear Higgs couplings, Proc. Sci. LL2024 (**2024**) 027.

[103] T. S. Roussy *et al.*, An improved bound on the electron's electric dipole moment, Science **381**, 46 (2023).

[104] W. Altmannshofer, S. Gori, N. Hamer, and H. H. Patel, Electron EDM in the complex two-Higgs doublet model, Phys. Rev. D **102**, 115042 (2020).

[105] I. Low, N. R. Shah, and X.-P. Wang, Higgs alignment and novel CP-violating observables in two-Higgs-doublet models, Phys. Rev. D **105**, 035009 (2022).

[106] T.-K. Chen, C.-W. Chiang, and I. Low, Simple model of dark matter and CP violation, Phys. Rev. D **105**, 075025 (2022).

[107] S. Banik and A. Crivellin, Explanation of the excesses in associated di-photon production at 152 GeV in 2HDM, J. High Energy Phys. 10 (2024) 203.

[108] S. Banik, G. Coloretti, A. Crivellin, and H. E. Haber, Correlating A $\to \gamma\gamma$ with electric dipole moments in the two Higgs doublet model in light of the diphoton excesses at 95 GeV and 152 GeV, Phys. Rev. D **111**, 075021 (2025).